Reactions of rhodium chloro complexes containing secondary phosphines with metal carbonyls $[M_3(CO)_{12}]$ (M = Fe, Ru): Synthesis and X-ray crystal structures of the metal clusters $[Ru_3Rh(CO)_7(\mu_3\text{-H})(\mu\text{-PBu}_2^t)_2(Bu_2^tPH)(\mu\text{-Cl})_2]$ and $[Ru_3Rh(CO)_8(\mu_3\text{-H})(\mu\text{-H})_2(\mu_3\text{-PBu}^t)(\mu\text{-PBu}_2^t)_2]$

Hans-Christian Böttcher *, Marion Graf, Kurt Merzweiler

Institut für Anorganische Chemie, Martin-Luther-Universität Halle-Wittenberg, Kurt-Mothes-Str. 2, D-06120 Halle Saale, Germany

Abstract

The reactions of $[RhCl(Bu_2^tPH)_3]$ (**1**) and $[\{RhCl(Bu_2^tPH)_2\}_2]$ (**2**), respectively, with the metal carbonyls $[M_3(CO)_{12}]$ (M = Fe, Ru) in refluxing toluene have been investigated. By using $[Fe_3(CO)_{12}]$ cluster degradation occurred and the known heterobimetallic complex $[FeRh(CO)_5(\mu\text{-PBu}_2^t)(Bu_2^tPH)]$ (**6**), in addition to the mononuclear compound $[Fe(CO)_4(Bu_2^tPH)]$ (**7**), was obtained. On the contrary, the reaction of **1** and **2**, respectively, with $[Ru_3(CO)_{12}]$ leads under oxidative addition to the trimetal core to the new heterometallic clusters $[Ru_3Rh(CO)_7(\mu_3\text{-H})(\mu\text{-PBu}_2^t)_2(Bu_2^tPH)(\mu\text{-Cl})_2]$ (**3**) in good yield beside $[Ru_3Rh(CO)_8(\mu_3\text{-H})(\mu\text{-H})_2(\mu_3\text{-PBu}^t)(\mu\text{-PBu}_2^t)_2]$ (**4**) and $[Ru_3(CO)_8(\mu\text{-H})_2(\mu_3\text{-PBu}^t)(Bu_2^tPH)]$ (**5**) as side products in low yields. The X-ray crystal structures of the butterfly configured tetrametal clusters **3** and **4** are reported. Compound **3** contains an elongated Ru–Ru hinge bond of 3.231(1) Å.

Keywords: Ruthenium; Rhodium; Carbonyl; Cluster; Phosphido-bridged; Crystal structure

1. Introduction

Complexes containing heteronuclear metal–metal bonds are of constant interest in view of site-selective reactivity and synergetic effects in catalytic reactions [1]. In a previous paper we reported on a new synthetic route to heteronuclear metal clusters by using oxidative addition reactions of metal halide complexes containing secondary phosphines to neutral metal carbonyl compounds. Thus, the thermolysis of $[IrCl(Bu_2^tPH)_3]$ with $[Ru_3(CO)_{12}]$ in toluene afforded the butterfly configuration of the metal cluster $[Ru_3Ir(CO)_7(\mu\text{-H})_2(\mu\text{-PBu}_2^t)_2(Bu_2^tPH)(\mu_3\text{-Cl})]$ in good yield amongst $[Ru_3(CO)_8(\mu\text{-H})_2(\mu_3\text{-PBu}^t)(Bu_2^tPH)]$ as minor product [2]. In this connection we were interested in analogous reactions using similar complexes as the starting materials, and herein we found that this reaction principle is also easy to apply to closely related rhodium compounds. In the present study, we are describing reac-

tions of metal carbonyls $[M_3(CO)_{12}]$ (M = Fe, Ru) with the complexes $[RhCl(Bu_2^tPH)_3]$ (**1**) and $[\{RhCl(Bu_2^tPH)_2\}_2]$ (**2**) respectively. The molecular structures of two products of the reactions with the $[Ru_3(CO)_{12}]$, namely $[Ru_3Rh(CO)_7(\mu_3\text{-H})(\mu\text{-PBu}_2^t)_2(Bu_2^tPH)(\mu\text{-Cl})_2]$ (**3**) and $[Ru_3Rh(CO)_8(\mu_3\text{-H})(\mu\text{-H})_2(\mu_3\text{-PBu}^t)(\mu\text{-PBu}_2^t)_2]$ (**4**) are reported.

2. Results and discussion

2.1. Reactions of metal halide complexes containing Bu_2^tPH with metal carbonyls $[M_3(CO)_{12}]$ (M = Fe, Ru)

At present, we are investigating reactions of neutral metal carbonyls with metal halide complexes of the late transition elements containing the bulky secondary phosphine Bu_2^tPH [2,3]. In this connection we can state that the trimetal core of $[Fe_3(CO)_{12}]$ is unsuitable for cluster condensation by thermolysis reactions with such metal halide complexes. As observed for the reaction of
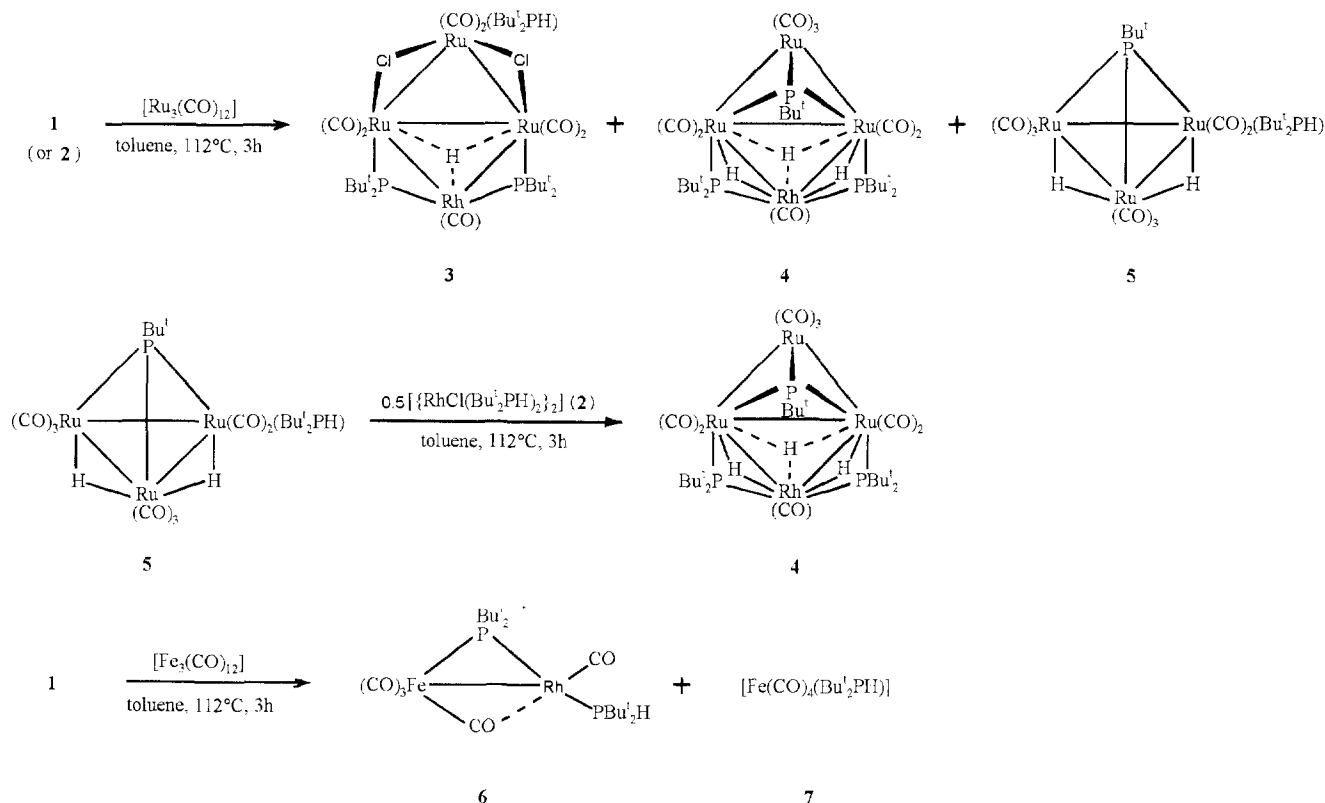
* Corresponding author.

[Fe$_3$(CO)$_{12}$] with [IrCl(Bu$^t_2$PH)$_3$] yielding the bimetallic system [FeIr(μ-CO)(CO)$_4$(μ-PBu$^t_2$)(Bu$^t_2$PH)] [3], also with the rhodium analogue [RhCl(Bu$^t_2$PH)$_3$] (1) cluster degradation occurred. Therefore, the reaction of 1 with [Fe$_3$(CO)$_{12}$] in refluxing toluene resulted in the formation of [FeRh(CO)$_5$(μ-PBu$^t_2$)(Bu$^t_2$PH)] (6) in yields of about 60% beside the complex [Fe(CO)$_4$(Bu$^t_2$PH)] (7) as minor product (Scheme 1). No other compounds could be detected by NMR spectroscopy.

On the contrary, the reaction of 1 with [Ru$_3$(CO)$_{12}$] under the same conditions leads to a mixture of products containing the new heteronuclear metal cluster [Ru$_3$Rh(CO)$_7$(μ_3-H)(μ-PBu$^t_2$)$_2$(Bu$^t_2$PH)(μ-Cl)$_2$] (3) as main product (48%). Interestingly, there is no evidence for a rhodium analogue of the compound [Ru$_3$Ir(CO)$_7$(μ-H)$_2$(μ-PBu$^t_2$)$_2$(Bu$^t_2$PH)(μ_3-Cl)] obtained as main product in a similar reaction of [IrCl(Bu$^t_2$PH)$_3$] with the trirutheniumdodecacarbonyl [2]. However, also in the present study the formation of [Ru$_3$(CO)$_8$(μ-H)$_2$(μ_3-PBu^t)(Bu$^t_2$PH)] (5) as a side product could be observed. The latter compound has been separated during purification of complex 3 by column chromatography on alumina, where 5 could be obtained at first in a yellow fraction with hexane as eluent. Subsequently, 3 was eluted in a red-brown band with hexane–diethyl ether (6:1). Furthermore, this fraction contained another product in very low yield which could be separated by fractional crystallization from

hexane at −30 °C. This compound was identified by a single X-ray diffraction study as [Ru$_3$Rh(CO)$_8$(μ_3-H)(μ-H)$_2$(μ_3-PBu^t)(μ-PBu$^t_2$)$_2$] (4) (see below). Surprisingly, the same results were observed in the analogous reaction of [Ru$_3$(CO)$_{12}$] with the complex [{RhCl(Bu$^t_2$PH)$_2$}$_2$] (2) (molar ratio 1:0.5), although only two phosphine ligands were present in the monomer unit instead of the required three for the synthesis of 3 and 4 respectively. The compounds 3 and 4 were fully characterized by microanalyses, spectroscopic means (IR, NMR and MS), and by single-crystal X-ray analyses.

The infrared spectrum of [Ru$_3$Rh(CO)$_7$(μ_3-H)(μ-PBu$^t_2$)$_2$(Bu$^t_2$PH)(μ-Cl)$_2$] exhibits only three ν(CO) absorption bands in the region characteristic of terminal carbonyl ligands, that is an indication of high molecular symmetry. The ^{1}H NMR spectrum of this compound shows signals corresponding to phosphine and phosphido ligands in a ratio of 1:2. Furthermore, a resonance signal at δ −19.33 was observed (multiplet, 1H). This signal can be assigned to the capping hydride ligand (see below) found in the X-ray analysis. In accordance with these data, the ^{31}P{^{1}H} NMR spectrum exhibits a signal at δ 350.12 (dd) indicating phosphido groups bridging metal–metal bonds and a corresponding signal at δ 45.57 (t) for a terminal bound phosphine (^3J(PP) = 16.8 Hz). Only a coupling between the phosphorus nuclei of the phosphido ligands with the rhodium nu-

Scheme 1.

cleus (J(RhP) = 100.4 Hz) could be observed. The mass spectrum of **3** shows the molecular ion peak and fragments resulting from successive carbonyl loss (see Section 4).

The infrared spectrum of **4** exhibits ν(CO) absorption bands corresponding to carbonyl ligands in a terminal coordination mode. The ^{31}P{^{1}H} NMR spectrum of this compound consists of a signal at δ 409.7 (dt, ^2J(PP) = 17.1 Hz, ^2J(RhP) = 8.5 Hz) and a corresponding resonance at δ 377.5 (dd, ^2J(PP) = 17.1 Hz, ^2J(RhP) = 93.9 Hz). These data indicate two chemically equivalent phosphorus nuclei of two phosphido bridges across metal–metal bonds which couple with a phosphorus nucleus of a phosphinidene ligand. In accordance with the ^{31}P NMR results, the proton NMR spectrum of **4** exhibits the corresponding signals for phosphinidene and phosphido ligands (relative areas 1:2). Furthermore, two different resonances at high field values were observed (δ −19.34, m, 2H; δ −21.36, m, 1H). According to the signal intensities, the latter resonance was assigned to the capping hydride ligand, which was located directly on the Ru$_2$Rh triangle during the single crystal X-ray study. Although no other hydrides were located additionally, we assume that two further hydride ligands occupy bridging sites across both Ru–Rh bonds and opposite to the phosphido groups. Since the metal cluster **4** contains a capping phosphinidene ligand like **5**, we assumed that this compound might be formed by condensation of **5** with a rhodium phosphine fragment. Therefore, we investigated the reaction of [Ru$_3$(CO)$_8$(μ-H)$_2$(μ_3-PBu^t)(Bu$^t_2$PH)] with **2** in refluxing toluene (Scheme 1). However, in this case the formation of **4** was also observed, though in very low yield (see Section 4). At present, we are searching for an improved synthetic way for this compound.

2.2. Molecular structure of [Ru$_3$Rh(CO)$_7$(μ_3-H)(μ-PBu$^t_2$)$_2$(Bu$^t_2$PH)(μ-Cl)$_2$] (3)

The molecular structure of **3** is shown in Fig. 1, selected bond lengths and angles are summarized in Table 1. The compound crystallizes from hexane in the monoclinic space group $P2_1/c$ with four molecules in the unit cell.

3 contains four metal atoms in a butterfly arrangement with the rhodium atom in one wing-tip site. Due to the very similar atomic scattering factors of Ru and Rh it is very difficult to distinguish between the Ru and Rh positions in the structure refinement. However, under consideration of the NMR spectra and the different coordination modes of the metal atoms, the assignment shown in Fig. 1 is the only reasonable one. A dihedral angle, defined as the δ angle [4], of 149° between the planes [Ru(1)–Ru(2)–Ru(3)] and [Ru(1)–Ru(2)–Rh] was determined (Fig. 2). Two equal Ru–Ru bond lengths
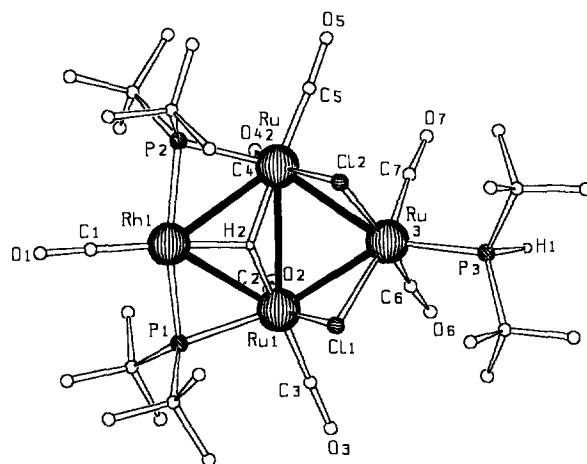
Fig. 1. The molecular structure of [Ru$_3$Rh(CO)$_7$(μ_3-H)(μ-PBu$^t_2$)$_2$(Bu$^t_2$PH)(μ-Cl)$_2$] (3).

[av. 2.954(1) Å] were found in the Ru$_3$ triangle, and the most interesting aspect in the molecular structure of **3** was the unusually long Ru(1)–Ru(2) hinge bond of 3.231(1) Å. Normally, the latter is too long to be an Ru–Ru single bond, (a 'normal' Ru–Ru bond length can be considered to be within the range 2.70–2.95 Å and, usually, elongated metal–metal bonds were often observed in formally electron-rich metal clusters [5]). A 62 cluster valence electron (c.v.e.) count is predicted for the butterfly configuration of metal frameworks, and

Table 1
Selected bond lengths (Å) and bond angles (deg) for 3

|			
Ru(1)–Ru(2)	3.231(1)	Ru(1)–Cl(1)	2.423(2)
Ru(2)–Ru(3)	2.956(1)	Ru(2)–Cl(2)	2.441(2)
Ru(3)–Ru(1)	2.953(1)	Ru(3)–Cl(1)	2.465(2)
Ru(1)–Rh	3.029(1)	Ru(3)–Cl(2)	2.445(2)
Ru(2)–Rh	2.998(1)	Ru(1)–P(1)	2.369(2)
Ru(1)–H(2)	1.820(5)	Ru(2)–P(2)	2.365(2)
Ru(2)–H(2)	1.881(5)	Ru(3)–P(3)	2.417(2)
Rh–H(2)	1.797(5)	Rh(1)–P(1)	2.304(2)
P(3)–H(1)	1.32(5)	Rh(1)–P(2)	2.299(2)
Ru(2)–C(4)	1.833(8)	Rh–C(1)	1.805(7)
Ru(2)–C(5)	1.864(9)	Ru(1)–C(2)	1.860(8)
Ru(3)–C(6)	1.839(8)	Ru(1)–C(3)	1.854(8)
Ru(3)–C(7)	1.860(9)		
Rh–Ru(1)–Ru(3)	108.1(1)	Ru(2)–Rh–P(2)	51.0(1)
Rh–Ru(2)–Ru(3)	108.8(1)	Ru(1)–P(1)–Rh	80.8(1)
Rh–Ru(1)–Ru(2)	57.1(1)	P(1)–Rh–P(2)	165.0(1)
Rh–Ru(2)–Ru(1)	58.0(1)	H(2)–Rh–C(1)	167.3(1)
Ru(1)–Ru(2)–Ru(3)	56.8(1)	Ru(2)–Ru(1)–P(1)	105.7(1)
Ru(2)–Ru(3)–Ru(1)	66.3(1)	Ru(1)–Ru(2)–P(2)	107.0(1)
Ru(1)–Rh–Ru(2)	64.8(1)	P(3)–Ru(3)–Cl(1)	98.2(1)
Ru(2)–P(2)–Rh	80.0(1)	P(3)–Ru(3)–Cl(2)	98.2(1)
Ru(1)–Ru(2)–Cl(2)	90.9(1)	Cl(1)–Ru(3)–Cl(2)	81.9(1)
Ru(2)–Ru(1)–Cl(1)	88.7(1)	Cl(2)–Ru(2)–Rh	104.6(1)
Cl(1)–Ru(1)–Rh	100.8(1)	Ru(1)–Cl(1)–Ru(3)	74.3(1)
P(3)–Ru(3)–Cl(1)	98.2(1)	Ru(2)–Cl(2)–Ru(3)	74.5(1)
P(3)–Ru(3)–Ru(2)	146.1(1)	P(3)–Ru(3)–Ru(1)	143.5(1)
P(3)–Ru(3)–Cl(2)	98.2(1)		
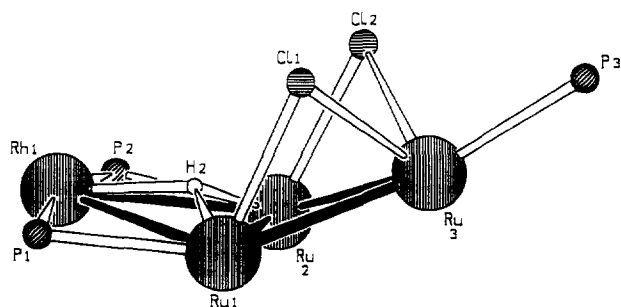
Fig. 2. Side-view on the butterfly configured central framework of **3** based on the X-ray data, showing the positions of the three donor P atoms, the two bridging chloride ions, the capping hydride and the Ru₃Rh metal core.

this criterion is fulfilled for complex **3** [considering that a bonding contact exists between Ru(1) and Ru(2)]. On the contrary, under the assumption of no significant bonding interaction between both metal atoms, the 18-electron rule would require an electron count of 64 c.v.e. for this cluster. However, that is not the case, and therefore an explanation for the lengthening of the Ru(1)–Ru(2) bond cannot be found by considering the electron count. Furthermore, a slight lengthening of both Ru–Rh bonds was observed. However, these distances (see Table 1) are comparable for instance with that reported for the compound [RuRh(μ-H)(H){ μ-CH(PPh$_2$)$_2$}(dppm)(COD)] (dppm = Ph$_2$PCH$_2$PPh$_2$, COD = 1.5-cyclooctadiene, Ru–Rh: 3.0306(6) Å) [6]. Moreover, it is well known that bridging hydride ligands cause lengthening of the corresponding metal–metal bonds.

The edges Ru(1)–Rh and Ru(2)–Rh, respectively, are bridged by a phosphido ligand, and the planes [Ru(1)–P(1)–Rh] and [Ru(2)–P(2)–Rh] are nearly coplanar. As expected for heterobimetallic systems, both phosphido bridges are slightly asymmetric, and as observed for the closely related system [Ru$_3$Ir(CO)$_7$(μ-H)$_2$(μ-PBu$^t_2$)$_2$(Bu$^t_2$PH)(μ_3-Cl)] [2], the Rh–(μ-P) distances are on an average of 0.067 Å shorter than the Ru–(μ-P) distances. Furthermore, a capping hydride with an asymmetric arrangement has been located directly on the Ru$_2$Rh triangle (see Table 1), and that is consistent with the observation of the ¹H NMR spectral resonance at δ −19.33 (C$_6$D$_6$). In contrast to the Ru$_3$Ir cluster mentioned before, which contains a μ_3-Cl ligand, two μ-Cl ligands were found in the Ru$_3$ triangle of **3**, and they occupy bridging sites across Ru(1)–Ru(3) and Ru(2)–Ru(3). The Ru–Cl distances can be compared to those found in ruthenium clusters containing chloride ligands, for instance [PPN]$_2$[Ru$_4$(μ-Cl)$_2$(CO)$_{11}$] (PPN = (PPh$_3$)$_2$N$^+$) [7] or [Ru$_3$(μ-Cl)$_2$(THF)$_2$(CO)$_8$] (THF = tetrahydrofuran) [8]. Up to now, there has been only some structural information on halide-bridged Ru$_3$ cores [9], and such a butterfly configured cluster containing phosphido- and chloro-bridges has been structurally characterized for the first time.
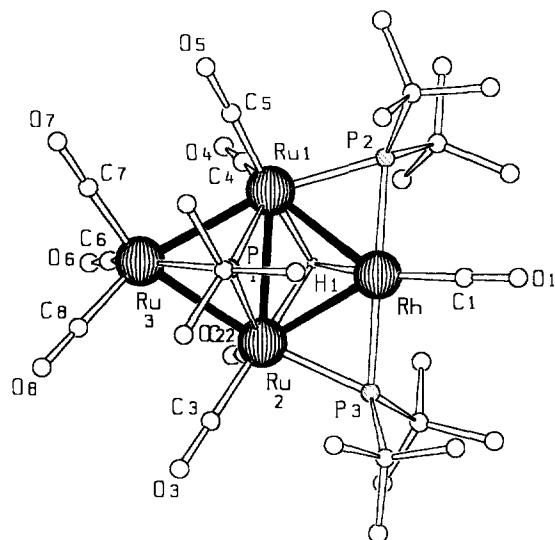

Fig. 3. The molecular structure of [Ru$_3$Rh(CO)$_8$(μ_3-H)(μ-H)$_2$(μ_3-PBu^t)(μ-PBu$^t_2$)$_2$] (**4**).

Furthermore, a phosphine ligand is coordinated to the Ru(3) atom in the wing-tip position. In accordance with the infrared data observed, only terminal carbonyl groups were found. Each ruthenium center bears two CO ligands, whereas the rhodium possesses only one. With regard to the bond angles found, the coordination sphere around the rhodium atom can be described as an almost square-planar arrangement.

2.3. Molecular structure of [Ru$_3$Rh(CO)$_8$(μ_3-H)(μ-H)$_2$(μ_3-PBu^t)(μ-PBu$^t_2$)$_2$] (4)

The molecule of **4** is shown in Fig. 3, selected bond lengths and angles are summarized in Table 2. The

Table 2
Selected bond lengths (Å) and bond angles (deg) for **4**

|			
Ru(1)–Rh	2.739(1)	Ru(1)–P(1)	2.357(1)
Ru(2)–Rh	2.733(1)	Ru(2)–P(1)	2.362(1)
Ru(1)–Ru(2)	2.942(1)	Ru(3)–P(1)	2.282(1)
Ru(2)–Ru(3)	2.860(1)	Ru(1)–P(2)	2.332(1)
Ru(3)–Ru(1)	2.883(1)	Rh–P(2)	2.334(1)
Rh–C(1)	1.843(4)	Ru(2)–P(3)	2.344(1)
Ru(1)–C(4)	1.932(4)	Rh–P(3)	2.331(1)
Ru(1)–C(5)	1.873(4)	Ru(3)–C(7)	1.876(5)
Ru(2)–C(2)	1.908(4)	Ru(3)–C(8)	1.890(5)
Ru(2)–C(3)	1.879(4)	Ru(3)–C(6)	1.977(5)
Ru(1)–H(2)	1.828	Ru(2)–H(2)	1.883
Rh–H(2)	1.797		
Ru(1)–P(1)–Ru(2)	77.1(1)	Ru(3)–Ru(2)–P(3)	163.3(1)
Ru(2)–P(1)–Ru(3)	76.0(1)	Ru(3)–Ru(1)–P(2)	166.0(1)
Ru(1)–P(1)–Ru(3)	76.8(1)	Ru(1)–Rh–P(3)	118.6(1)
Ru(2)–Ru(1)–P(2)	109.0(1)	Ru(2)–Rh–P(2)	116.2(1)
Ru(1)–Ru(2)–P(3)	110.8(1)	P(3)–Rh–P(2)	153.6(1)
Rh–Ru(1)–Ru(3)	112.1(1)	Rh–Ru(2)–Ru(3)	113.0(1)
Ru(1)–Rh–Ru(2)	65.1(1)	Ru(3)–Ru(2)–Ru(1)	59.6(1)
Ru(1)–Ru(3)–Ru(2)	61.6(1)	Ru(3)–Ru(1)–Ru(2)	58.8(1)
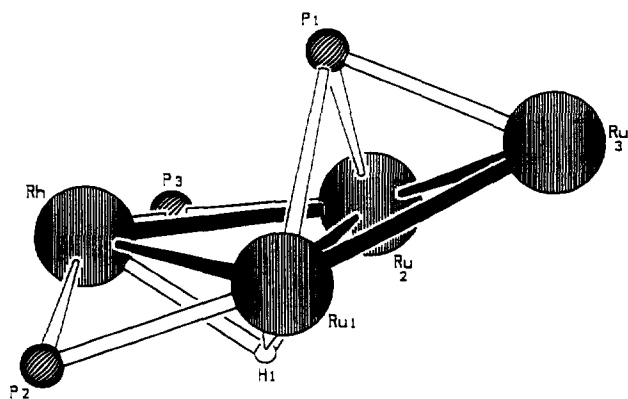
Fig. 4. Side-view on the butterfly configured central framework of **4** based on the X-ray data, showing the positions of the three donor P atoms, the capping hydride and the Ru_3Rh metal core.

compound crystallizes from hexane in the monoclinic space group $P2_1/c$ with four molecules in the unit cell.

As observed for **3**, even in the case of **4**, a butterfly configured tetrametal cluster core with the rhodium atom in one wing-tip site was found. The dihedral angle δ between the two planes [Ru(1)–Ru(2)–Ru(3)] and [Ru(1)–Ru(2)–Rh] is 155° (Fig. 4); therefore, the butterfly core is more folded than that in the Ru_3Ir cluster mentioned above (166°), but less folded than that in the tetrametal unit of **3** (149°). The five metal–metal bonds in **4** lie in the expected range for single bonds (av. Ru–Ru: 2.895(1); av. Ru–Rh: 2.736(1) Å). The closed Ru_3 triangle is μ_3-capped by a phosphinidene ligand, and the edges Ru(1)–Rh and Ru(2)–Rh in the Ru_2Rh wing are bridged by a μ-PBu$_2^t$ ligand, respectively. These phosphido ligands lie nearly in the same plane of the Ru_2Rh triangle [Ru(3)–Ru(1)–P(2), 166.0(1); Ru(3)–Ru(2)–P(3), 163.3(1)°]. The phosphinidene cape exhibits an asymmetric arrangement [Ru(1)–P(1), 2.357(1); Ru(2)–P(1), 2.362(1) and Ru(3)–P(1), 2.282(1) Å], and such an observation was also made in [Ru$_3$Ir(CO)$_7$(μ-H)$_2$(μ-PBu$_2^t$)$_2$(Bu$_2^t$PH)(μ_3-Cl)] [2]. In contrast to the structure found for **3**, the phosphido bridges are symmetrically arranged in **4**, e.g. the Ru–(μ-P) and Rh–(μ-P) distances, respectively, exhibit nearly the same value (av. 2.335(1) Å). Furthermore, a capping hydride could be located directly on the Ru_2Rh triangle [Ru(1)–H(2), 1.828; Ru(2)–H(2), 1.883; Rh–H(2), 1.797 Å]. In accordance with the infrared investigations, only carbonyl groups in a terminal coordination mode were found. The Rh center bears only one carbonyl ligand, and with regard to the hydrides bridging both Ru–Rh bonds (see above), for the rhodium the coordination number five results.

3. Conclusions

In the present study we could realize cluster condensations by oxidative addition reactions of metal halide

complexes containing secondary phosphines to the trimetal core of [Ru$_3$(CO)$_{12}$]. This reaction principle works for [IrCl(Bu$_2^t$PH)$_3$] as well as for the analogous rhodium compounds **1** and **2**, respectively. In the former case the product [Ru$_3$Ir(CO)$_7$(μ-H)$_2$(μ-PBu$_2^t$)$_2$(Bu$_2^t$PH)(μ_3-Cl)] results, while the latter reactions lead to the clusters [Ru$_3$Rh(CO)$_7$(μ_3-H)(μ-PBu$_2^t$)$_2$(Bu$_2^t$PH)(μ-Cl)$_2$] (**3**) and [Ru$_3$Rh(CO)$_8$(μ_3-H)(μ-H)$_2$(μ_3-PBu^t)(μ-PBu$_2^t$)$_2$] (**4**). Generally, the discussion of a metal–metal bond between Ru(1) and Ru(2) in **3** (hinge bond) is complicated. This circumstance refers to one of the most interesting aspects of tetranuclear transition metal clusters, namely the structural diversity exhibited by molecules with formal 62- or 64-electron counts [5,10]. Thus, two possible descriptions of the bonding situation can be made: (a) **3** is a 62-electron cluster with a considerably elongated hinge bond (18-electron rule fulfilled), or (b) no bonding contact between Ru(1)–Ru(2) is assumed, therefore an electronically unsaturated structure results (62 c.v.e. instead of the required 64 to obey the 18-electron rule). With regard to the 16-electron rule (square-planar arrangement at the formally rhodium(I) center), the second description gives a more satisfactory explanation of the electron count in this molecule. The latter aspect is in accordance with the metal–metal bond distances and the electron count observed in the butterfly clusters [Ru$_3$Ir(CO)$_7$(μ-H)$_2$(μ-PBu$_2^t$)$_2$(Bu$_2^t$PH)(μ_3-Cl)] and **4**, respectively: both complexes exhibit five metal–metal distances in the range expected for single bonds, the coordination number at the rhodium is five, and the 18-electron rule is fulfilled. Therefore, the more reasonable description of **3** is a structure without bonding interaction between Ru(1) and Ru(2). Generally, a number of factors including the electronic structure and skeletal electron count of the butterfly, steric effects between metal fragments, and coordinating properties of the constituent ligands might be expected to influence geometrical features of the tetrametal core [10].

4. Experimental

All reactions were carried out under dry argon, using standard Schlenk techniques. Solvents were dried over molecular sieves or sodium–benzophenone ketyl, and were distilled under nitrogen prior to use. Starting materials were either commercially available or were prepared according to literature procedures. The syntheses of [RhCl(Bu$_2^t$PH)$_3$] and [{RhCl(Bu$_2^t$PH)$_2$}$_2$], respectively, were described elsewhere [11,12]. IR spectra were obtained using a Mattson 5000 instrument. ^{1}H NMR and ^{31}P NMR spectra were recorded on the spectrometer Bruker AC 200 (^{1}H at 200.1 MHz, ^{31}P NMR at 81.0 MHz). The mass spectra were obtained on a Hitachi Perkin Elmer RMU 6, Nermag R30-10 instru-

ment. Elemental analyses: Analytisches Laboratorium des Pharmazeutischen Institutes der Martin-Luther-Universität Halle-Wittenberg.

4.1. Reaction of [RhCl(Bu$_2^t$PH)$_3$] (1) with [Fe$_3$(CO)$_{12}$]

A mixture of 1 (577 mg, 1 mmol) and [Fe$_3$(CO)$_{12}$] (504 mg, 1 mmol) was heated in refluxing toluene (40 ml) for 3 h. After cooling to room temperature and removal of the solvent the residue was extracted three times with 20 ml portions of pentane. The volume of the combined extracts was reduced to 10 ml and separated by column chromatography on alumina with hexane as eluent. At first a yellow band containing [Fe(CO)$_4$(Bu$_2^t$PH)] (7) (detected by ^{31}P NMR, not isolable as solid, see Ref. [2]) was obtained. A second orange band contains [FeRh(CO)$_5$(μ-PBu$_2^t$)(Bu$_2^t$PH)] (6) which was crystallized as an orange solid after reducing the solvent to 10 ml and cooling at −30 °C overnight (yield: 342 mg, 58%); spectroscopic data for 6 see Refs. [12,13].

4.2. Reaction of 1 with [Ru$_3$(CO)$_{12}$]; synthesis of 3 and 4

A mixture of 1 (577 mg, 1 mmol) and [Ru$_3$(CO)$_{12}$] (640 mg, 1 mmol) was heated in refluxing toluene (40 ml) for 3 h. After cooling to room temperature and

removal of the solvent the residue was extracted three times with 20 ml portions of pentane. The volume of the combined extracts was reduced to 10 ml and separated by column chromatography on alumina with hexane as eluent. At first a yellow band containing 5 was obtained (61 mg, 8% isolated yield, characterized by NMR [2]). Further elution with a mixture of hexane–diethyl ether (6:1) afforded a red-brown fraction containing 3 and 4. These complexes were separated by fractional crystallization from hexane at −30 °C (yields: 534 mg 3, 48%; 30 mg 4, 3%).

3. Anal. Found: C, 33.51; H, 5.23; Cl, 6.19%; M, 1111.88 (calc.). C$_{31}$H$_{56}$Cl$_2$O$_7$P$_3$RhRu$_3$ calc.: C, 33.52; H, 5.08, Cl, 6.38%. IR: ν(CO) (CsBr): 2034m; 2006s, sh; 1960s cm^{-1}. ^{1}H NMR δ (C$_6$D$_6$): 4.64 (d, J(PH) = 333.3 Hz, 1H, Bu$_2^t$PH), 1.44 (dt, N = 76.0 Hz, 36H, μ-PBu$_2^t$), 1.22 (d, ^{3}J(PH) = 14.3 Hz, 18H, Bu$_2^t$PH), −19.33 (m, 1H, μ_3-H). ^{31}P{^{1}H} NMR δ (C$_6$D$_6$): 350.12 (dd, ^{3}J(PP) = 16.8 Hz, J(RhP) = 100.4 Hz, μ-PBu$_2^t$), 45.57 (t, ^{3}J(PP) = 16.8 Hz, Bu$_2^t$PH). MS: 1113, M$^+$; 1085, [M − CO]$^+$; 1057, [M − 2CO]$^+$; 1029, [M − 3CO]$^+$; 1001, [M − 4CO]$^+$; 973, [M − 5CO]$^+$; 57, [C$_4$H$_9$]$^+$, 100%.

4. Anal. Found: C, 33.35; H, 5.02%; M, 1013.88 (calc.). C$_{28}$H$_{48}$O$_8$P$_3$RhRu$_3$ calc.: C, 33.14; H, 4.77%. IR: ν(CO) (CsBr): 2005s, 1984m, 1960vs, 1943s cm^{-1}. ^{1}H NMR δ (C$_6$D$_6$): 1.32 (d, ^{3}J(PH) = 18.0 Hz, 9H, μ_3-PBu^t), 1.21 (dt, N = 74.5 Hz, 36H, μ-PBu^t), −19.34

Table 3
Crystal data and structure refinement for 3 and 4

Identification code	3	4
Empirical formula	C$_{31}$H$_{56}$Cl$_2$O$_7$P$_3$RhRu$_3$	C$_{28}$H$_{48}$O$_8$P$_3$RhRu$_3$
Formula weight	1111.88	1013.88
Temperature	R.T.	R.T.
Wavelength	0.71073 Å	0.71073 Å
Crystal system	monoclinic	monoclinic
Space group	P2$_1$/c	P2$_1$/c
Unit cell dimensions	a = 21.497(3) Å	a = 17.830(4) Å
	b = 12.3264(2) Å	b = 11.530(2) Å
	c = 17.661(3) Å	c = 20.409(5) Å
	β = 109.51(2)°	β = 115.51(2)°
Volume	4411.2(10) Å^3	3786.6(14) Å^3
Z	4	4
Density (calculated)	1.672 g cm^{-3}	1.775 g cm^{-3}
Absorption coefficient	1.643 mm^{-1}	1.770 mm^{-1}
F(000)	2216	2008
θ range for data collection	2.31 to 25.0°	2.67 to 28.04°
Index ranges	28 ≤ h ≤ 28, −16 ≤ k ≤ 16, −23 ≤ l ≤ 23	−23 ≤ h ≤ 23, −15 ≤ k ≤ 15, −26 ≤ l ≤ 26
Reflections collected	42265	31779
Independent reflections	7772	9024
Refinement method	Full-matrix least squares on F^2 all non-hydrogen atoms	
	anisotropic	anisotropic
Data/restraints/parameters	7772/0/432	9024/0/572
Goodness-of-fit on F^2	1.011	1.021
Final R indices [I > 2σ(I)]	R1 = 0.0454, wR2 = 0.0838	R1 = 0.0342, wR2 = 0.0630
R indices (all data)	R1 = 0.0949, wR2 = 0.0998	R1 = 0.0620, wR2 = 0.0709
Largest diff. peak and hole	0.706 and −0.587 e Å^{-3}	0.757 and −0.894 e Å^{-3}

(m, 2H, μ-H), −21.36 (m, 1H, μ_3-H). ^{31}P{^{1}H} NMR δ (C$_6$D$_6$): 409.66 (dt, ^2J(PP) = 17.1 Hz, ^2J(RhP) = 8.5 Hz, μ_3-PBu^t), 377.51 (dd, ^2J(PP) = 17.1 Hz, J(RhP) = 93.9 Hz, μ-PBu^t). MS: 1014, M^+; 986, [M − CO]$^+$; 958, [M − 2CO]$^+$; 930, [M − 3CO]$^+$; 902, [M − 4CO]$^+$; 874, [M − 5CO]$^+$; 57, [C$_4$H$_9$]$^+$, 100%.

Similar results were observed by using the complex [{RhCl(Bu$^t_2$PH)$_2$}$_2$] (2).

4.3. Reaction of 5 with 2

A mixture of 5 (191 mg, 0.25 mmol) and 2 (108 mg, 0.13 mmol) was heated in refluxing toluene (30 ml) for 3 h. After cooling to room temperature and removal of the solvent, the residue was extracted three times with 15 ml portions of hexane. The volume of the combined extracts was reduced to 10 ml and purified by column chromatography on alumina with hexane as eluent. A red-brown band containing the complexes 3 and 4 was obtained. These two compounds were separated by fractional crystallization at −30 °C from hexane, where 4 crystallized first (yield about 3%).

5. X-ray structure determinations

Crystals of 3 and 4, respectively, suitable for X-ray diffraction were grown by cooling a hexane solution (−30 °C). For the data collection the diffractometer Stoe-IPDS was used. The structures were solved by direct methods and refined on F^2 (program systems: SHELXS-86, SHELXL-93 [14]). A summary of crystal data along with details of the structure determinations are given in Table 3. Full details of the structure determinations have been deposited at the Fachinformationszentrum Karlsruhe, Gesellschaft für wissenschaftlich-technische Information mbH, D-76344 Eggenstein-Leopoldshafen, Germany, from where this material may be obtained on quoting the full literature citation and the reference number *CSD 59367.

References

[1] B.H.S. Thimmappa, *Coord. Chem. Rev.*, *143* (1995) 1 and references cited therein.
[2] H.-C. Böttcher, M. Graf and K. Merzweiler, *J. Organomet. Chem.*, in press.
[3] H.-C. Böttcher, M. Graf and K. Merzweiler, *J. Organomet. Chem.*, *525* (1996) 191.
[4] C. Mealli and D.M. Proserpio, *J. Am. Chem. Soc.*, *112* (1990) 5484.
[5] J.F. Corrigan, M. Dinardo, S. Doherty, G. Hogarth, Y. Sun, N.J. Taylor and A.J. Carty, *Organometallics*, *13* (1994) 3572 and references cited therein.
[6] H. Benlaarab, B. Chaudret, F. Dahan and R. Poilblanc, *J. Organomet. Chem.*, *320* (1987) C51.
[7] G. Lavigne, N. Lugan, P. Kalck, J.M. Soulié, O. Lerouge, J.Y. Saillard and J.F. Halet, *J. Am. Chem. Soc.*, *114* (1992) 10669.
[8] H. Cho and B.R. Whittlesey, *Inorg. Chem.*, *32* (1993) 3789.
[9] A.J. Deeming, in E.W. Abel, F.G.A. Stone and G. Wilkinson (eds.), *Comprehensive Organometallic Chemistry II*, Vol. 7, Pergamon, Oxford, 1995, Chapter 12, p. 683.
[10] E. Sappa, A. Tiripicchio, A.J. Carty and G.E. Toogood, *Prog. Inorg. Chem.*, *35* (1987) 437.
[11] C. Masters and B.L. Shaw, *J. Chem. Soc.*, (1971) 3679.
[12] B. Walther, H.-C. Böttcher, M. Scheer, G. Fischer, D. Fenske and G. Süss-Fink, *J. Organomet. Chem.*, *437* (1992) 307.
[13] A.M. Arif, D.E. Heaton and R.A. Jones, *Polyhedron*, *10* (1991) 543.
[14] G.M. Sheldrick, SHELXS-86, SHEXL-93, *Programs for Crystal Structure Determination*, University of Göttingen, 1986, 1993.